Electronic Supplementary Information (ESI)

Metal-free polycycloaddition of aldehyde-activated internal diynes and diazides toward post-functionalizable poly(formyl-1,2,3-triazole)s

Baixue Li,[†] Anjun Qin*,[†] and Ben Zhong Tang*,[†,‡]

[†]State Key Laboratory of Luminescent Materials and Devices, Guangdong Provincial Key Laboratory of Luminescence from Molecular Aggregates, Center for Aggregation-Induced Emission, South China University of Technology, Guangzhou 510640, China.

[‡]Department of Chemistry, Hong Kong Branch of Chinese National Engineering Research Center for Tissue Restoration and Reconstruction, Institute for Advanced Study, and Department of Chemical and Biological Engineering, The Hong Kong University of Science & Technology, Clear Water Bay, Kowloon, Hong Kong, China.

Table of Content

Monomer synthesis. The aldehyde-activated internal diynes, named 3,3'-(9,9-dibutyl-9H-fluorene-2,7-diyl)dipropiolaldehyde (**1a**) and 3,3'-(9,9-dimethyl-9H-fluorene- 2,7-diyl)dipropiol-aldehyde (**1b**) were prepared according to the published procedures.[1,2] The azides monomers, 1,4-bis((6-azidohexyl)oxy)benzene (**2a**), 1,2-bis(4-(azidomethyl)phenyl)-1,2-diphenylethene (**2b**), bis(4-azidophenyl)- methane (**2c**) and 1,2-bis(4-((6-azidohexyl) oxy)phenyl)-1,2-diphenylethene (**2d**) were prepared according to the previous reports.[3-6] The detailed synthetic routes are shown in Schemes S1 and S2.

3,3'-(9,9-Dibutyl-9H-fluorene-2,7-diyl)dipropiolaldehyde (1a): ^{1}H NMR (500 MHz, $CDCl_3$), δ (TMS, ppm): 9.46, 7.77, 7.75, 7.64, 7.61, 1.99, 1.10, 0.68, 0.55. ^{13}C NMR (125 MHz, $CDCl_3$), δ (TMS, ppm): 176.77, 151.89, 142.97, 132.92, 128.08, 121.03, 118.98, 96.01, 89.39, 55.62, 39.98, 26.04, 23.05, 13.90.

3,3'-(9,9-Dimethyl-9H-fluorene-2,7-diyl)dipropiolaldehyde (1b): ^{1}H NMR (500 MHz, $CDCl_3$), δ (TMS, ppm): 9.45, 7.78, 7.76, 7.70, 7.65, 7.63, 1.51. ^{13}C NMR (125 MHz, $CDCl_3$), δ (TMS, ppm): 176.74, 154.58, 141.11, 133.06, 128.05, 121.28, 119.16, 95.75, 89.33, 47.34, 26.84.

1,4-Bis((6-azidohexyl)oxy)benzene (2a): ^{1}H NMR (500 MHz, $CDCl_3$), δ (TMS, ppm): 6.81, 3.90, 3.27, 1.77, 1.62, 1.46. ^{13}C NMR (125 MHz, $CDCl_3$), δ (TMS, ppm): 153.23, 115.30, 68.36, 51.37, 29.32, 28.77, 26.63, 25.77.

1,2-Bis(4-(azidomethyl)phenyl)-1,2-diphenylethene (2b): ^{1}H NMR (500 MHz, $CDCl_3$), δ (TMS, ppm): 7.11, 7.03, 4.26. ^{13}C NMR (125 MHz, $CDCl_3$), δ (TMS, ppm): 143.77, 143.26, 140.81, 133.53, 131.83, 131.24, 128.02, 126.83, 54.62.

Bis(4-azidophenyl)methane (2c): ^{1}H NMR (500 MHz, $CDCl_3$), δ (TMS, ppm): 7.14, 6.96, 3.92. ^{13}C NMR (125 MHz, $CDCl_3$), δ (TMS, ppm): 138.26, 137.76, 130.22, 119.47, 40.82.

1,2-Bis(4-((6-azidohexyl)oxy)phenyl)-1,2-diphenylethene (2d): ^{1}H NMR (500 MHz, $CDCl_3$), δ (TMS, ppm): 7.12-7.00, 6.94-6.89, 6.65-6.60, 3.90-3.86, 3.29-3.26, 1.78-1.73, 1.66-1.60, 1.50-1.43. ^{13}C NMR (125 MHz, $CDCl_3$), δ (TMS, ppm): 157.58, 144.41, 139.77, 136.43, 132.64, 131.54, 127.68, 126.28, 113.66, 67.63, 51.54, 31.08, 29.31, 28.94, 26.68, 25.87.

Post-modification model reactions. Compounds **6**-A/**6**-B and cis-**7**/trans-**7** were prepared according to the published procedures.[7,8] The detailed synthetic routes are shown in Scheme S4 and S5.

6-A: ^{1}H NMR (500 MHz, $CDCl_3$), δ (TMS, ppm): 8.43, 7.49-6.61, 5.51, 2.57, 2.49, 1.56, 1.29, 1.25, 0.87.

6-B: ^{1}H NMR (500 MHz, $CDCl_3$), δ (TMS, ppm): 8.51, 7.69-6.64, 6.17, 2.62, 2.49, 1.62, 1.26, 0.88.

cis-**7**: ^{1}H NMR (500 MHz, $CDCl_3$), δ (TMS, ppm): 7.52-7.45, 7.27, 7.15-7.05, 6.76 (d, *J*=12 Hz, 1H), 5.41 (d, *J*=12 Hz, 1H).

trans-**7**: ^{1}H NMR (500 MHz, $CDCl_3$), δ (TMS, ppm): 7.54-7.49, 7.28, 7.15-7.03, 6.28 (d, *J*=16 Hz, 1H).

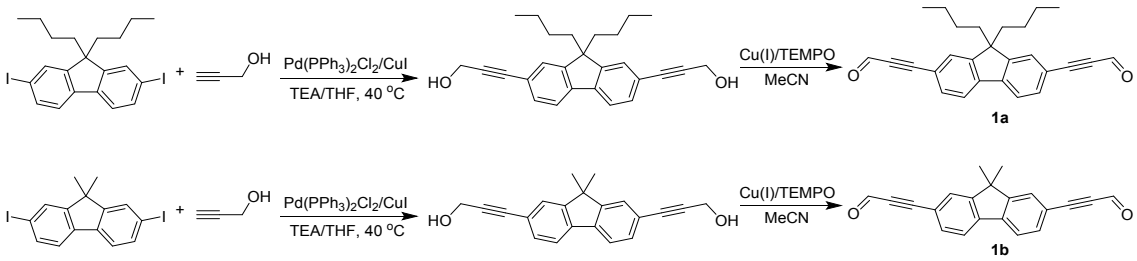

Scheme S1 Synthesis of **1a** and **1b**.

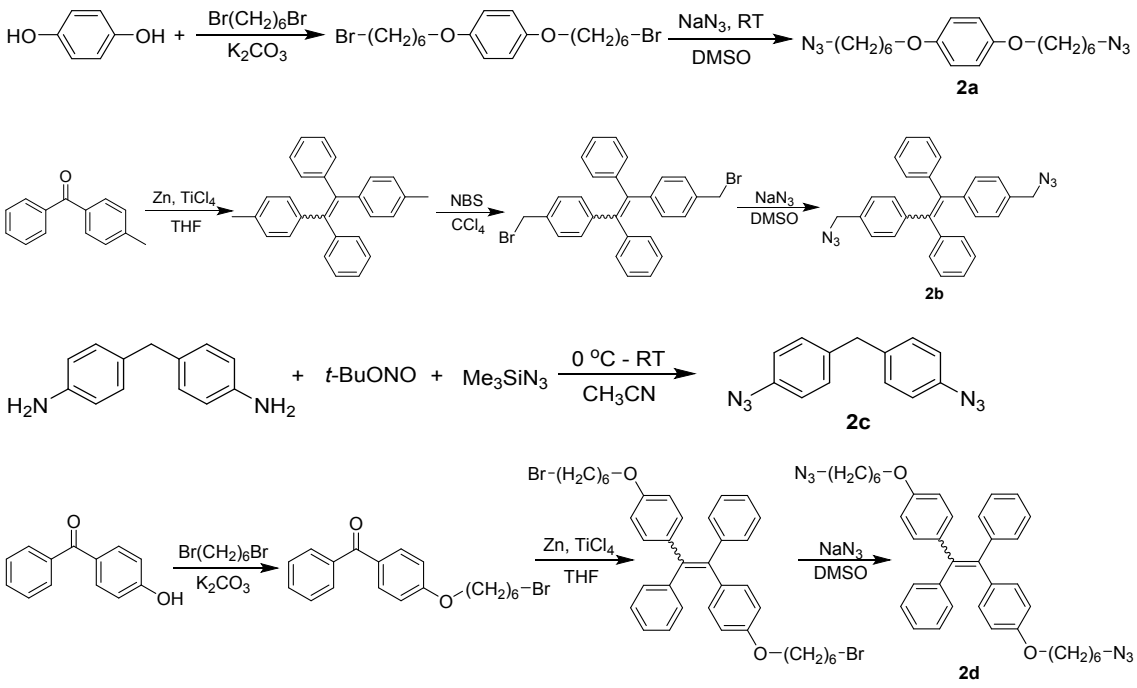

Scheme S2 Synthesis of **2a-2d**.

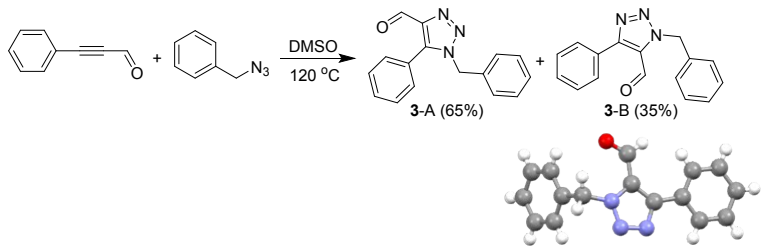

Scheme S3 Synthesis of **3**-A and **3**-B.

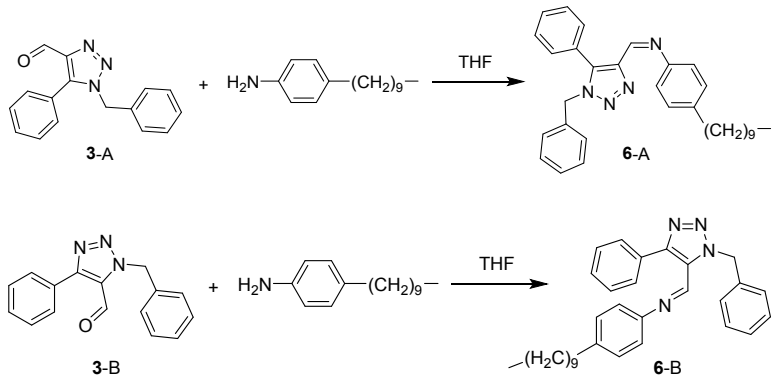

Scheme S4 Synthesis of **6**-A and **6**-B.

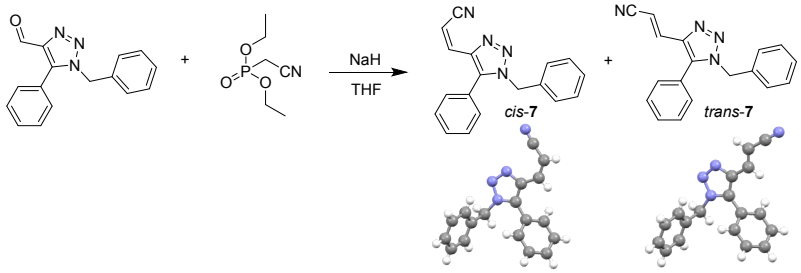

Scheme S5 Synthesis of *cis*-**7** and *trans*-**7**.

Table S1 Effect of solvent on the polymerization of **1a** and **2a**[a]

entry	solvent	yield (%)	M_w[b]	PDI[b]	F_A[c] (%)
1	DMSO	85	16 360	1.55	71
2	DMF	80	14 580	1.48	68
3	1,4-dioxane	79	12 950	1.41	64
4	toluene	71	15 300	1.47	61

[a] Carried out at 120 °C for 3 h under nitrogen at a monomer concentration of 0.5 M, [**1a**] = [**2a**]. [b] Estimated by advanced polymer chromatography (APC) using THF as an eluent on the basis of a polystyrene (PS) calibration; M_w = weight-average molecular weight; polydispersity index (PDI) = M_w/M_n; M_n = number-average molecular weight. [c] Fraction of structure A in the polymers determined by ^{1}H NMR.

Table S2 Effect of reaction temperature on the polymerization of **1a** and **2a**[a]

entry	T (°C)	yield (%)	M_w[b]	PDI[b]
1	80	52	4410	1.22
2	100	63	11 090	1.37
3	120	80	15 190	1.48
4	140	87	43 350	2.09
5	150	83	53 110	2.55

[a] Carried out in DMSO for 3 h under nitrogen at a monomer concentration of 0.5 M, [**1a**] = [**2a**]. [b] Estimated by APC using THF as an eluent on the basis of a PS calibration; M_w = weight-average molecular weight; PDI = M_w/M_n; M_n = number-average molecular weight.

Table S3 Time course of the polymerization of **1a** and **2a**[a]

entry	t (h)	yield (%)	M_w[b]	PDI[b]
1	1.0	76	23 440	1.71
2	1.5	88	48 920	2.21
3	2.0	89	54 550	2.29
4	3.0	90	58 690	2.39

[a] Carried out in DMSO at 150 °C under nitrogen at a monomer concentration of 0.5 M, [**1a**] = [**2a**]. [b] Estimated by APC using THF as an eluent on the basis of a PS calibration; M_w = weight-average molecular weight; PDI = M_w/M_n; M_n = number-average molecular weight.

Table S4 Effect of monomer concentration on the polymerization of **1a** and **2a**[a]

entry	C (M)	yield (%)	M_w[b]	PDI[b]
1	0.10	75	9730	1.33
2	0.20	80	18 470	1.59
3	0.33	85	37 420	1.94
4[c]	0.50	89	54 550	2.29
5	1.00	gelled	-	-

[a] Carried out in DMSO at 150 °C under nitrogen for 2 h, [**1a**] = [**2a**]. [b] Estimated by APC using THF as an eluent on the basis of a PS calibration; M_w = weight-average molecular weight; PDI = M_w/M_n; M_n = number-average molecular weight. [c] Data taken from Table S3, entry 3.

Table S5 Crystal data and structure refinement of model compound **3-B**

Number	CCDC 1958959
Empirical formula	$C_{16}H_{13}N_3O$
Formula weight	263.29
Temperature	120(10) K
Wavelength	1.54184 Å
Crystal system	monoclinic
Space group	P 1 21/c 1
Unit cell dimensions	a = 13.1254(7) Å α = 90.00 °
	b = 8.1029(4) Å β = 109.249 °
	c = 12.6860(7) Å γ = 90.00 °
Volume	1273.78(12) $Å^3$
Z	4
Density (calculated)	1.373 mg/m^3
Absorption coefficient	0.713 mm^{-1}
F(000)	552
Crystal size	0.07 × 0.05 × 0.05 mm^3
Theta range for data collection	3.567 to 67.097 °
Index ranges	-15<=h<=14, -6<=k<=9, -14<=l<=15
Reflections collections	5898
Independent reflections	2269 [R(int) = 0.0240]
Completeness to theta = 66.97°	99.9%
Absorption correction	multi-scan
Max. and min. transmission	1.00000 and 0.71569
Data / restraints / parameters	2269 / 0 / 181
Goodness-of-fit on F^2	1.077
Final R indices [I>2sigma(I)]	R1 = 0.0437, wR2 = 0.1074
R indices (all data)	R1 = 0.0450, wR2 = 0.1083
Largest diff. peak and hole	0.256 and -0.397 e.$Å^{-3}$

Table S6 Crystal data and structure refinement of model compound *cis*-**7**

Number	CCDC 1958962
Empirical formula	$C_{18}H_{14}N_4$
Formula weight	286.33
Temperature	293(2) K
Wavelength	0.71073 Å
Crystal system	triclinic
Space group	P-1
Unit cell dimensions	a = 9.1045(15) Å α = 110.846 °
	b = 9.4078(14) Å β = 92.668 °
	c = 9.9658(17) Å γ = 107.055 °
Volume	751.7(2) $Å^3$
Z	2
Density (calculated)	1.265 mg/m^3
Absorption coefficient	0.078 mm^{-1}
F(000)	300
Crystal size	0.22 × 0.19 × 0.16 mm^3
Theta range for data collection	2.79 to 25.10 °
Index ranges	-10<=h<=10, -11<=k<=11, -11<=l<=11
Reflections collections	10178
Independent reflections	2573 [R(int) = 0.0586]
Completeness to theta = 25.10°	95.9%
Absorption correction	multi-scan
Max. and min. transmission	0.9876 and 0.9830
Data / restraints / parameters	2573 / 0 / 199
Goodness-of-fit on F^2	1.001
Final R indices [I>2sigma(I)]	R1 = 0.0679, wR2 = 0.1817
R indices (all data)	R1 = 0.0944, wR2 = 0.1939

Table S7 Crystal data and structure refinement of model compound *trans*-**7**

Number	CCDC 1958961
Empirical formula	$C_{18}H_{14}N_4$
Formula weight	286.33
Temperature	300(2) K
Wavelength	0.71073 Å
Crystal system	monoclinic
Space group	P2(1)/c
Unit cell dimensions	a = 11.0650(8) Å α = 90.00 °
	b = 15.5926(12) Å β = 108.433 °
	c = 9.3078(6) Å γ = 90.00 °
Volume	1523.50(19) $Å^3$
Z	4
Density (calculated)	1.248 mg/m^3
Absorption coefficient	0.077 mm^{-1}
F(000)	600
Crystal size	0.24 × 0.18 × 0.15 mm^3
Theta range for data collection	2.61 to 26.00 °
Index ranges	-13<=h<=13, -19<=k<=19, -11<=l<=11
Reflections collections	18156
Independent reflections	2989 [R(int) = 0.0540]
Completeness to theta = 26.00°	99.5%
Absorption correction	multi-scan
Max. and min. transmission	0.9885 and 0.9817
Data / restraints / parameters	2989 / 0 / 199
Goodness-of-fit on F^2	1.005
Final R indices [I>2sigma(I)]	R1 = 0.0537, wR2 = 0.1403
R indices (all data)	R1 = 0.0821, wR2 = 0.1721

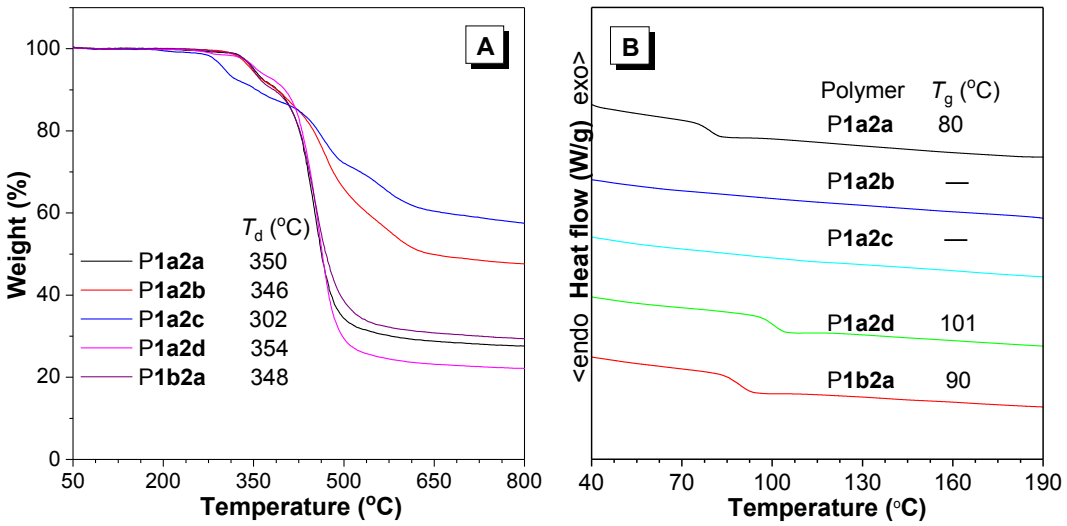

Fig. S1 TGA (A) and DSC (B) curves of P**1a2a**-P**1b2a** at a heating rate of 20 °C min^{-1} under nitrogen. T_d presents temperature of 5% weight loss.

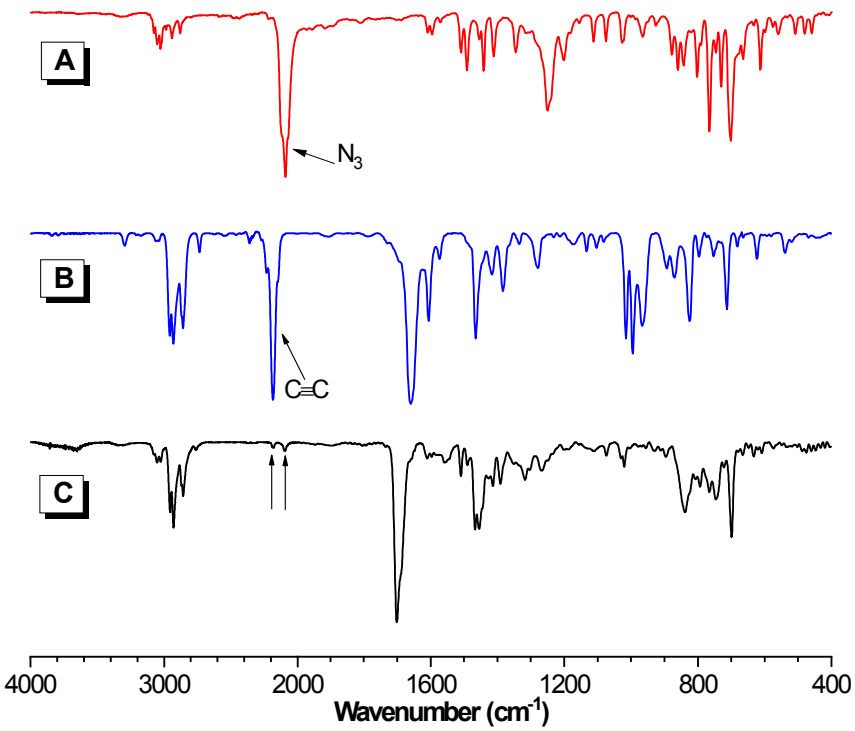

Fig. S2 FT-IR spectra of **2b** (A), **1a** (B) and P**1a2b** (C).

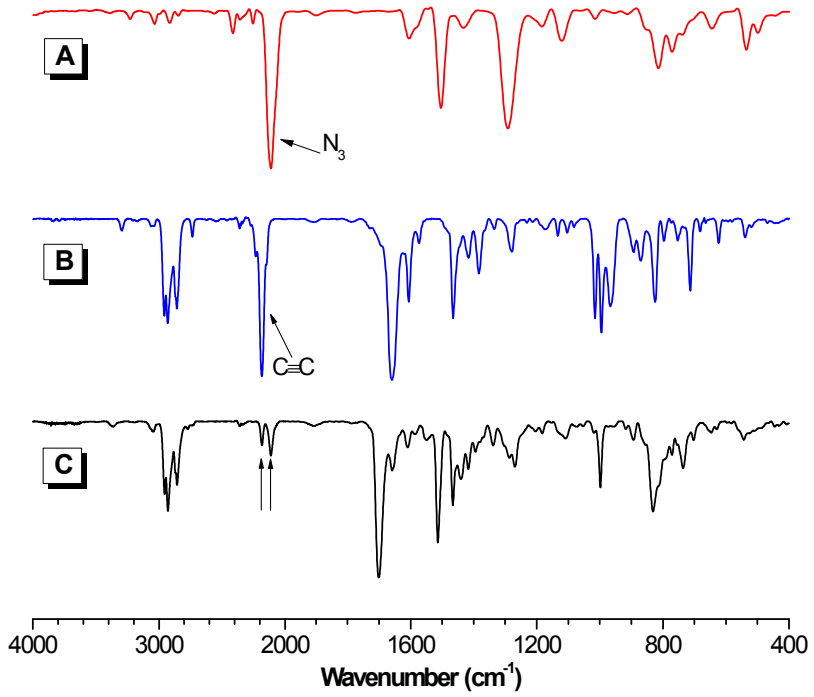

Fig. S3 FT-IR spectra of **2c** (A), **1a** (B) and P**1a2c** (C).

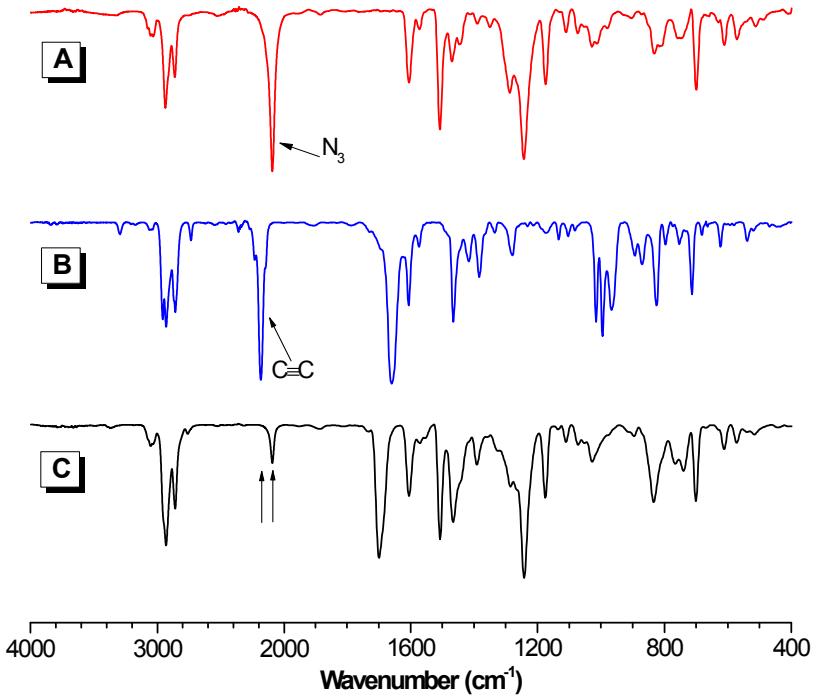

Fig. S4 FT-IR spectra of **2d** (A), **1a** (B) and P**1a2d** (C).

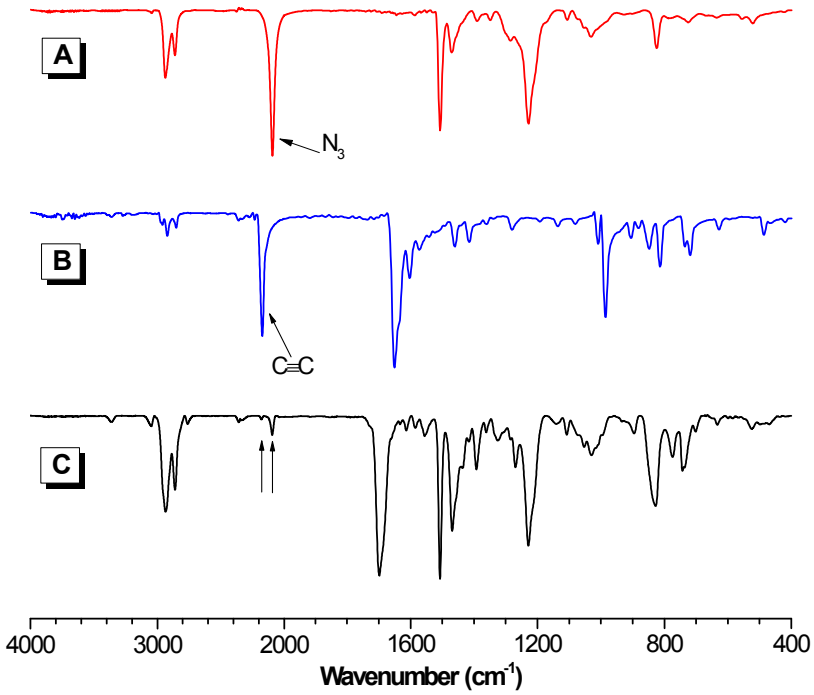

Fig. S5 FT-IR spectra of **2a** (A), **1b** (B) and P**1b2a** (C).

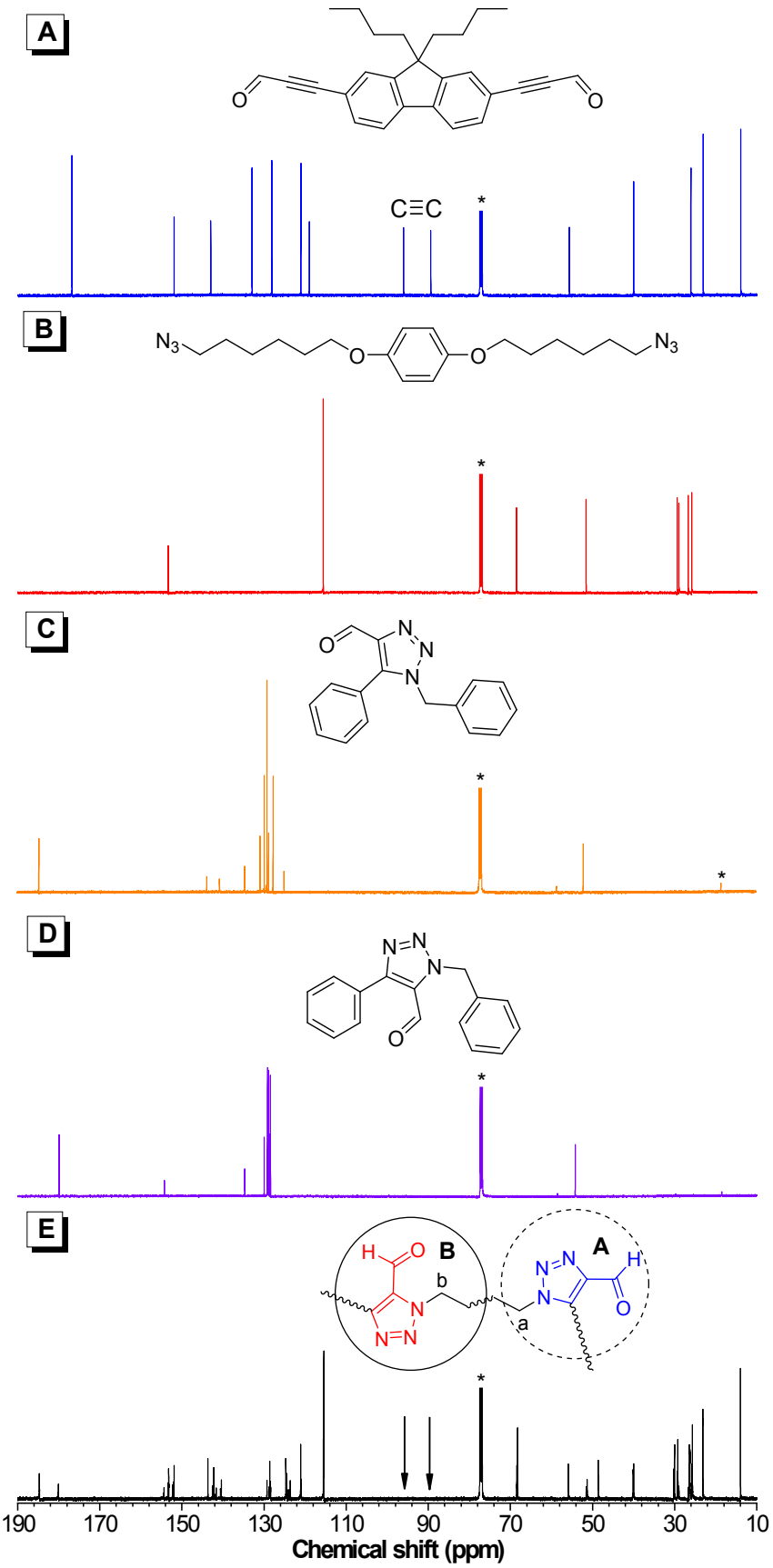

Fig. S6 ^{13}C NMR spectra of **1a** (A), **2a** (B), **3**-A (C), **3**-B (D) and P**1a2a** (E) in $CDCl_3$. The solvent peaks are marked with asterisks.

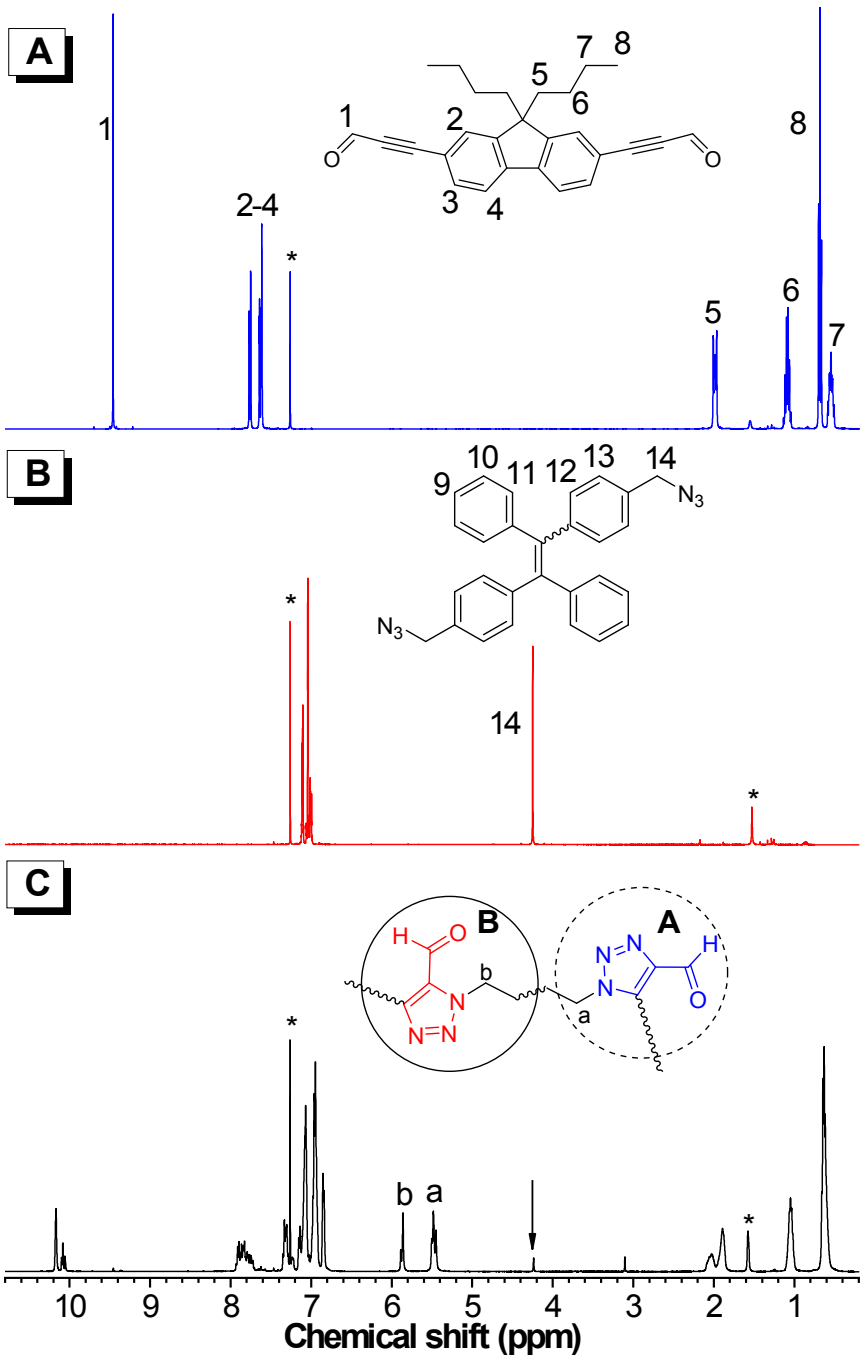

Fig. S7 ^{1}H NMR spectra of **1a** (A), **2b** (B) and P**1a2b** (C) in $CDCl_3$. The solvent peaks are marked with asterisks.

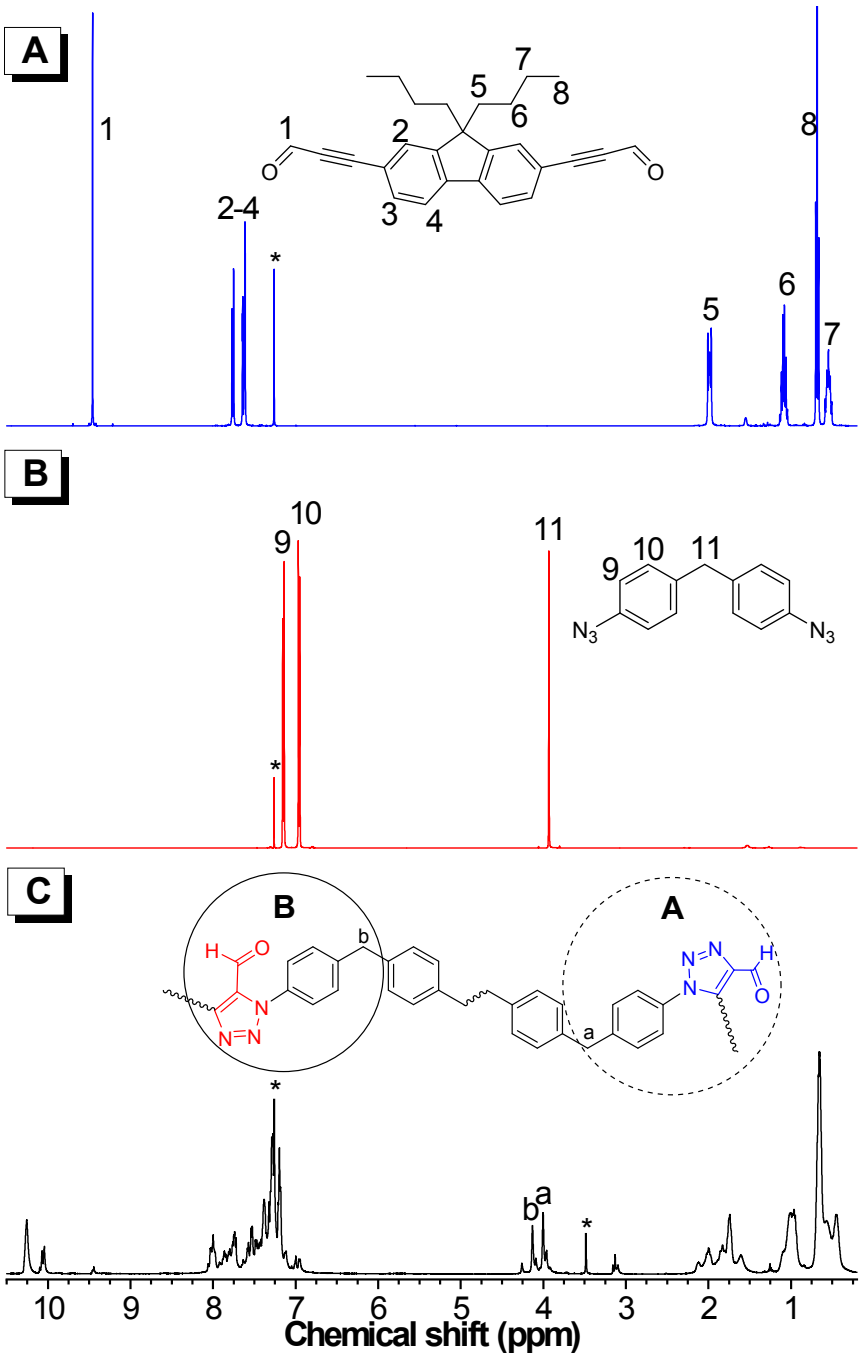

Fig. S8 ^{1}H NMR spectra of **1a** (A), **2c** (B) and P**1a2c** (C) in $CDCl_3$. The solvent peaks are marked with asterisks.

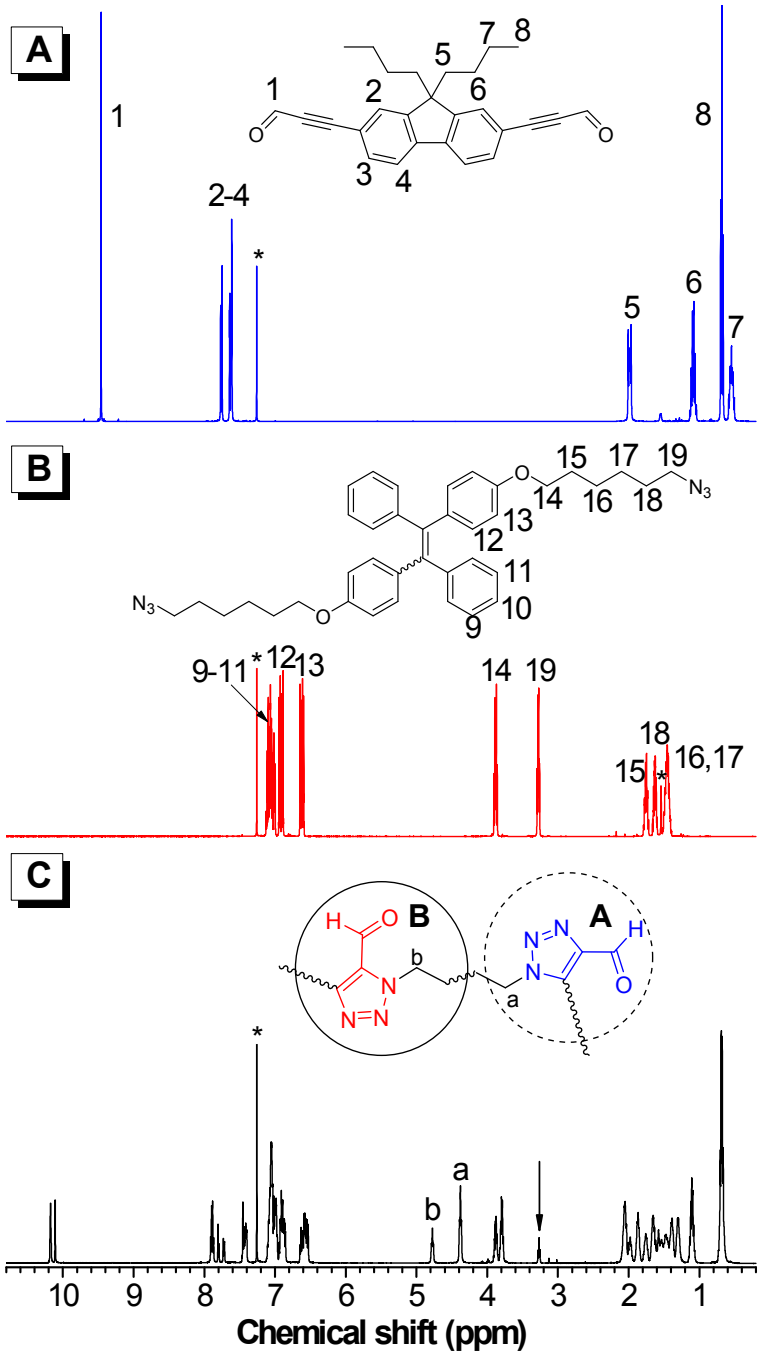

Fig. S9 ^{1}H NMR spectra of **1a** (A), **2d** (B) and P**1a2d** (C) in $CDCl_3$. The solvent peaks are marked with asterisks.

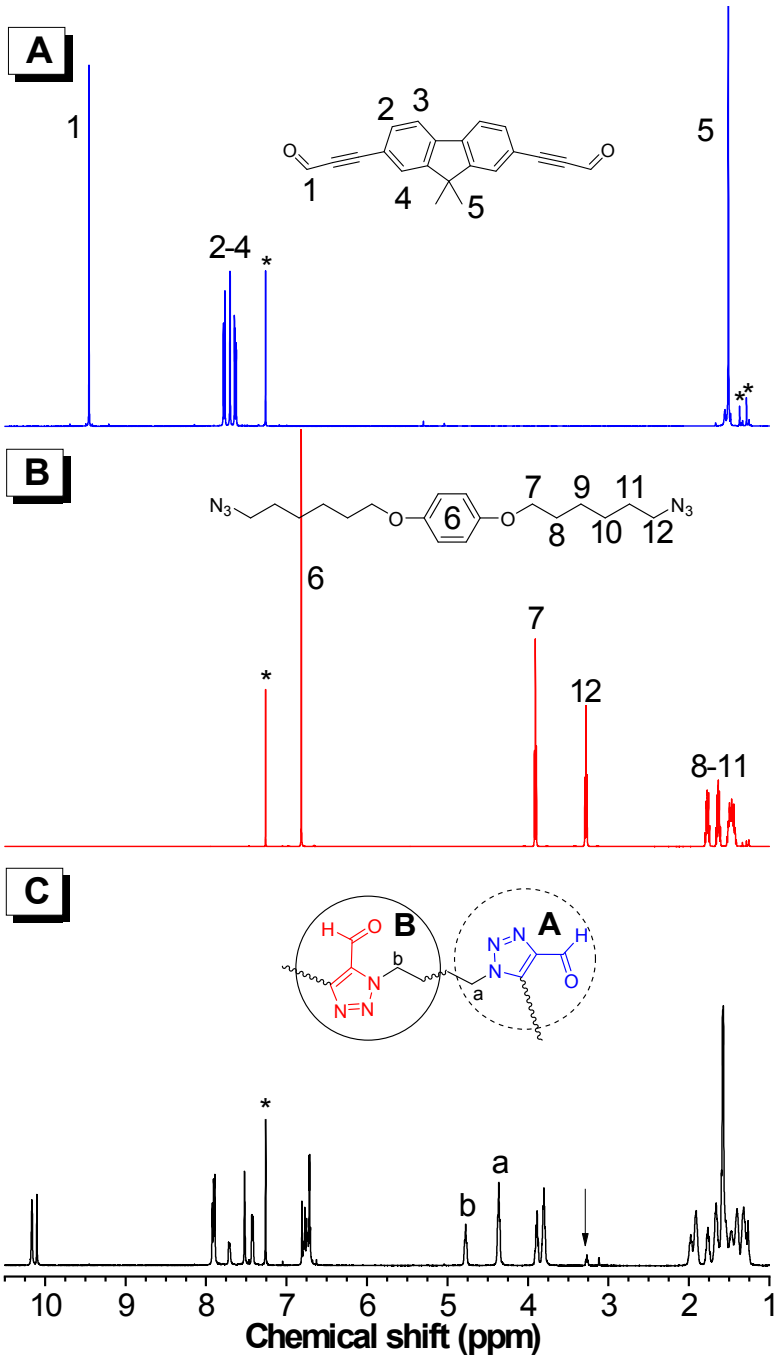

Fig. S10 ^{1}H NMR spectra of **1b** (A), **2a** (B) and P**1b2a** (C) in $CDCl_3$. The solvent peaks are marked with asterisks.

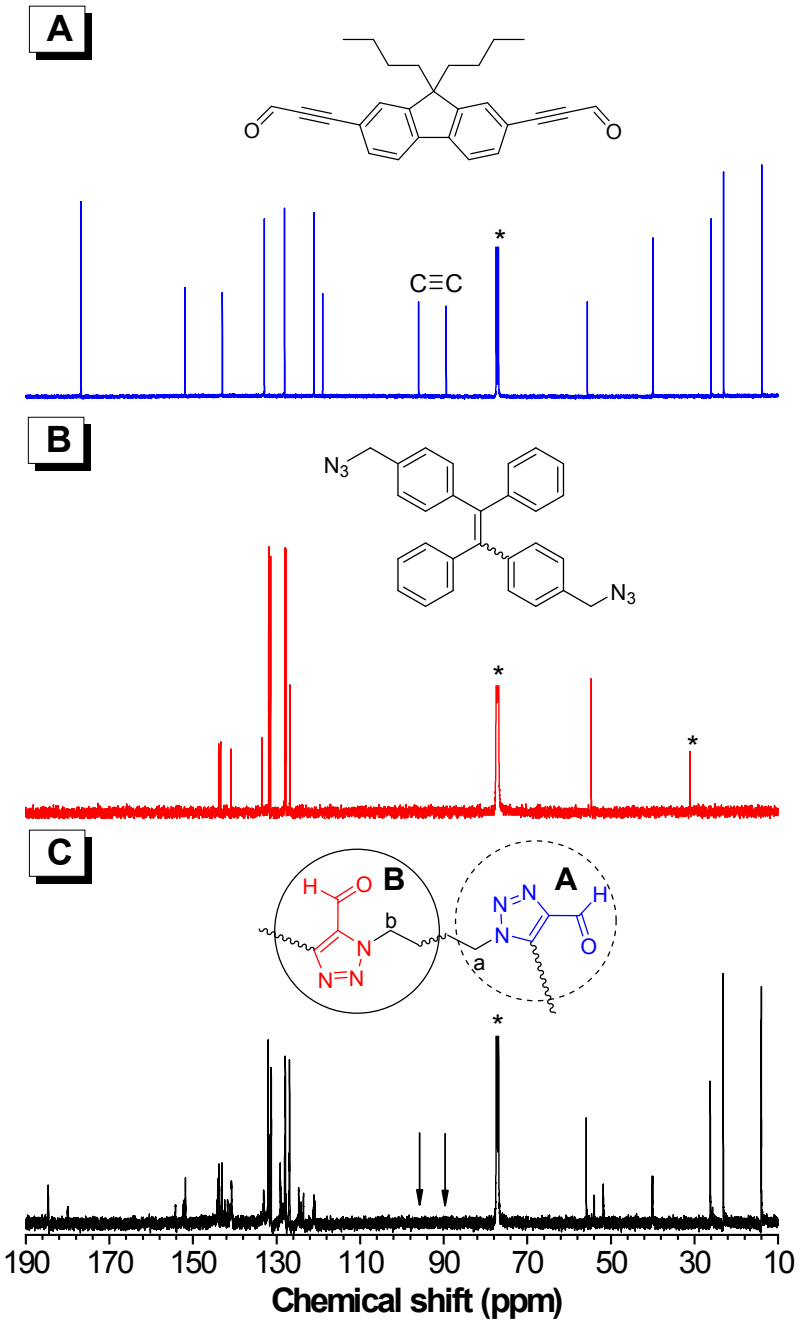

Fig. S11 ^{13}C NMR spectra of **1a** (A), **2b** (B) and P**1a2b** (C) in $CDCl_3$. The solvent peaks are marked with asterisks.

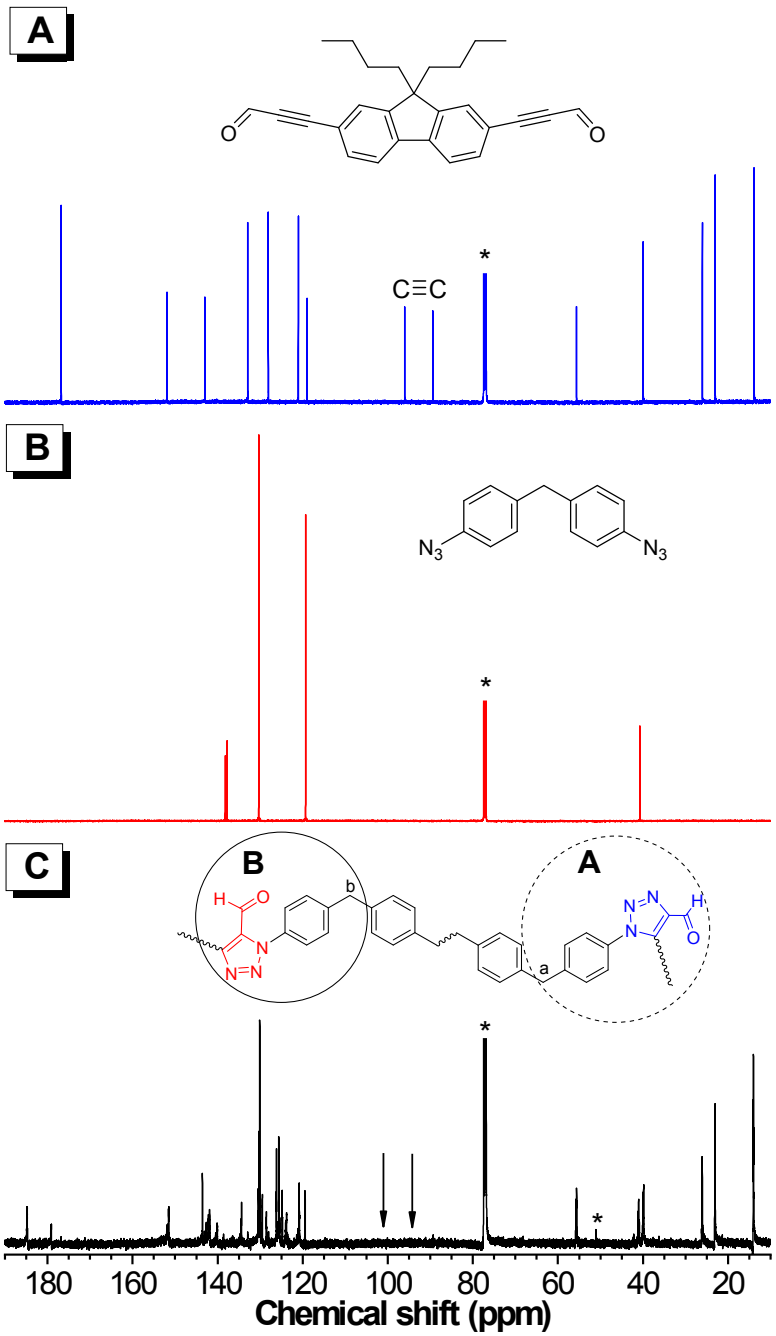

Fig. S12 ^{13}C NMR spectra of **1a** (A), **2c** (B) and P**1a2c** (C) in $CDCl_3$. The solvent peaks are marked with asterisks.

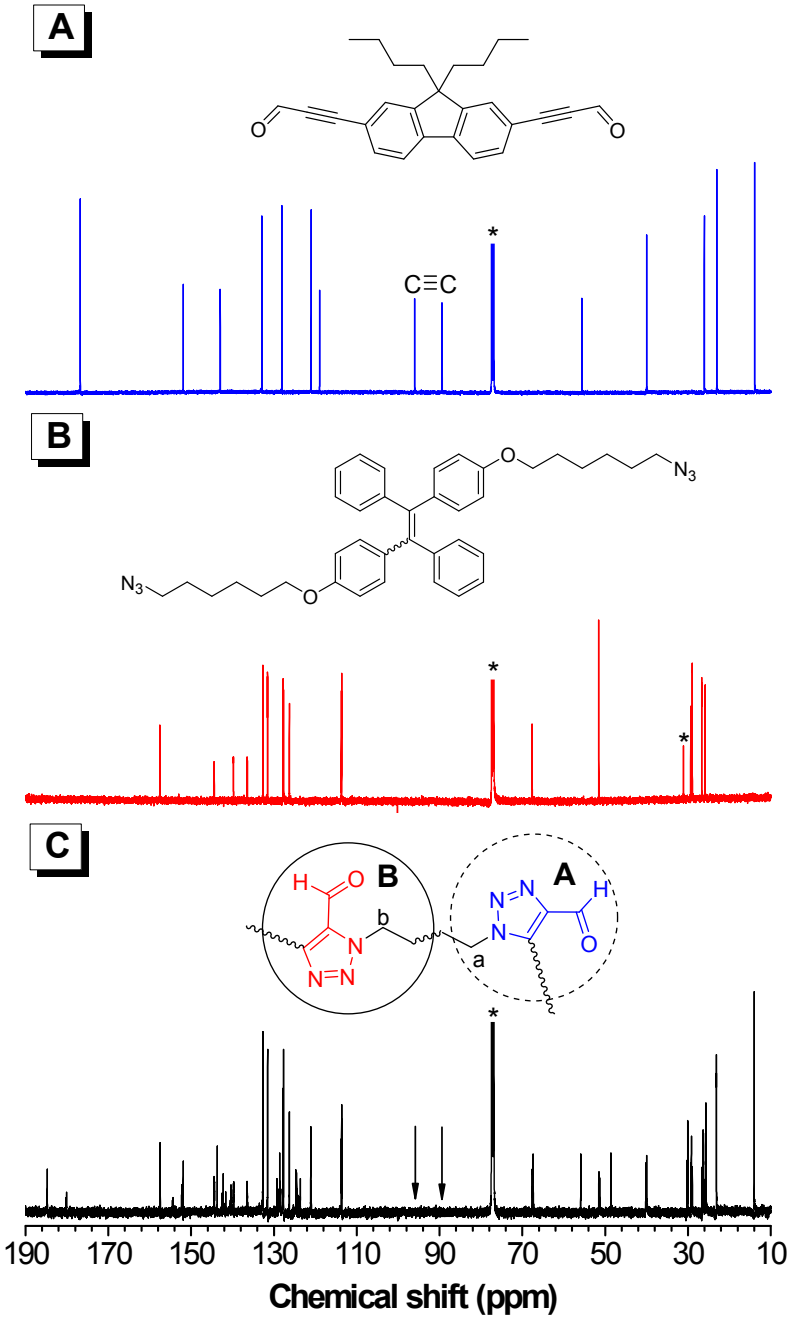

Fig. S13 ^{13}C NMR spectra of **1a** (A), **2d** (B) and P**1a2d** (C) in $CDCl_3$. The solvent peaks are marked with asterisks.

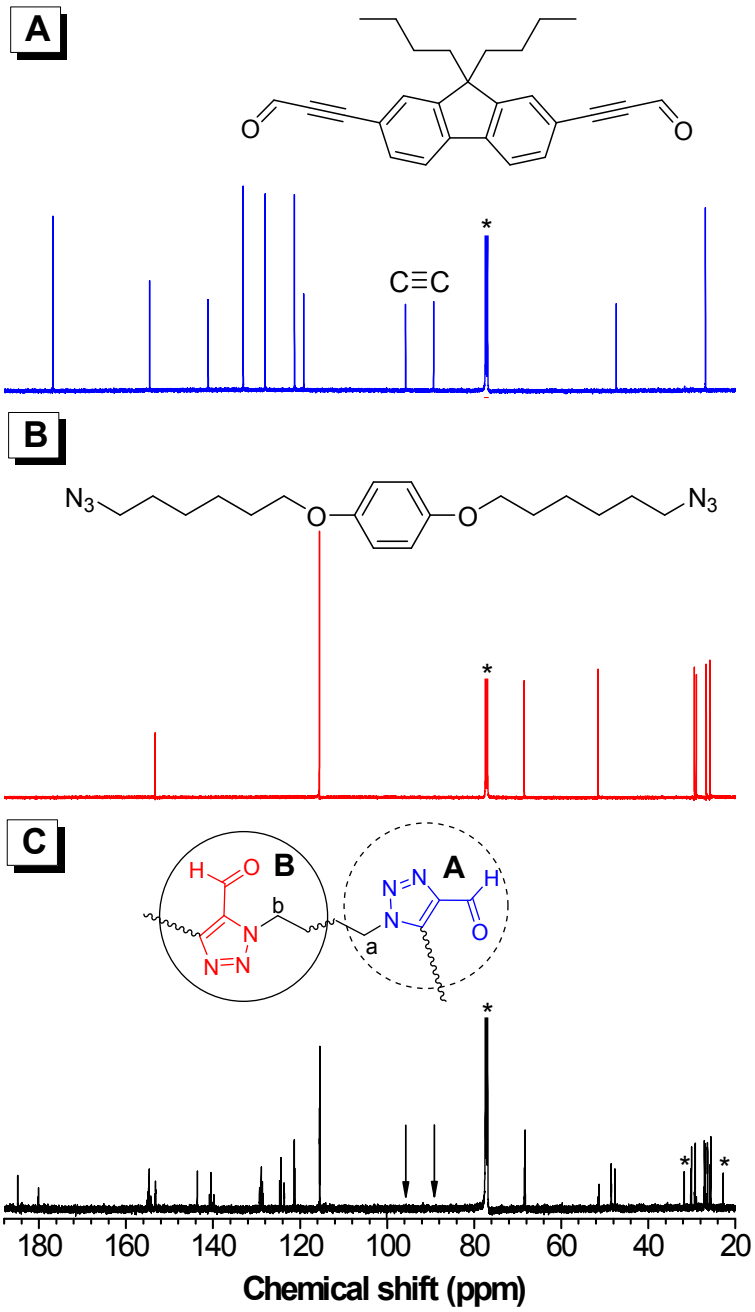

Fig. S14 ^{13}C NMR spectra of **1b** (A), **2a** (B) and P**1b2a** (C) in $CDCl_3$. The solvent peaks are marked with asterisks.

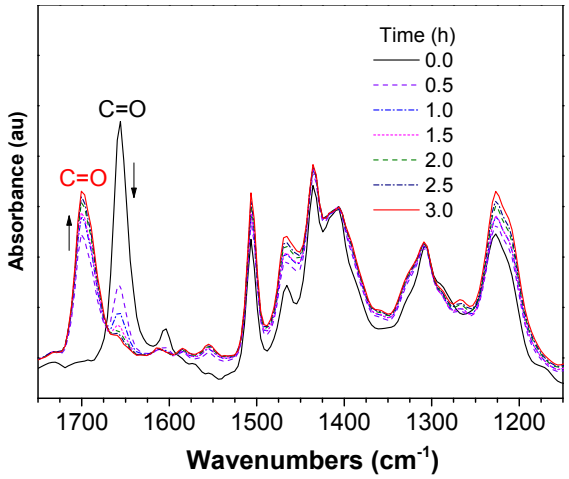

Fig. S15 The in situ IR spectra of the polymerization solution of **1a** and **2a** at 150 °C within 3 h.

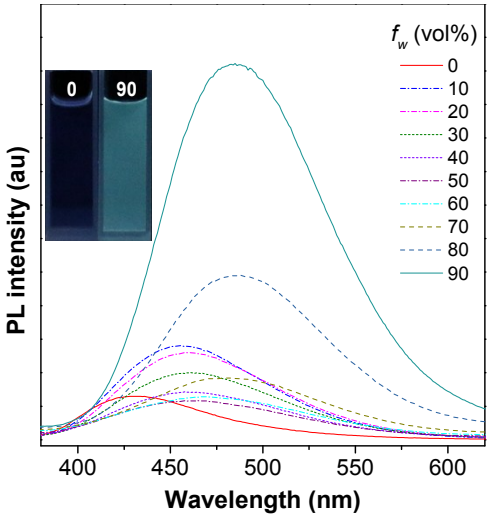

Fig. S16 PL spectra of P**1a2d** in THF and THF/water mixtures with different water fractions. Concentrations: 10^{-5} M, λ_{ex} = 323 nm. Inset: photograph taken under illumination of hand-held UV lamp.

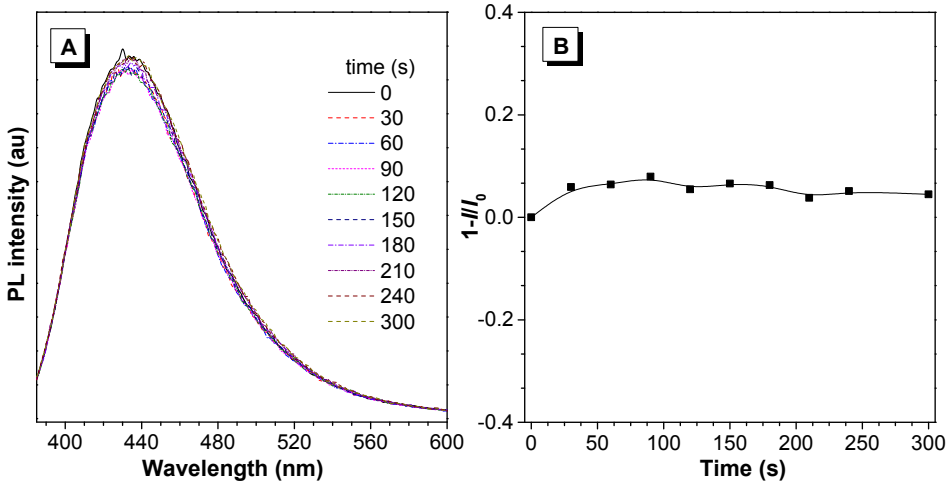

Fig. S17 Changes of PL spectrum (A) and the plot of normalized changes in PL intensity (1-I/I_0) of P**1a2a** treated with hydrazine in THF solutions.

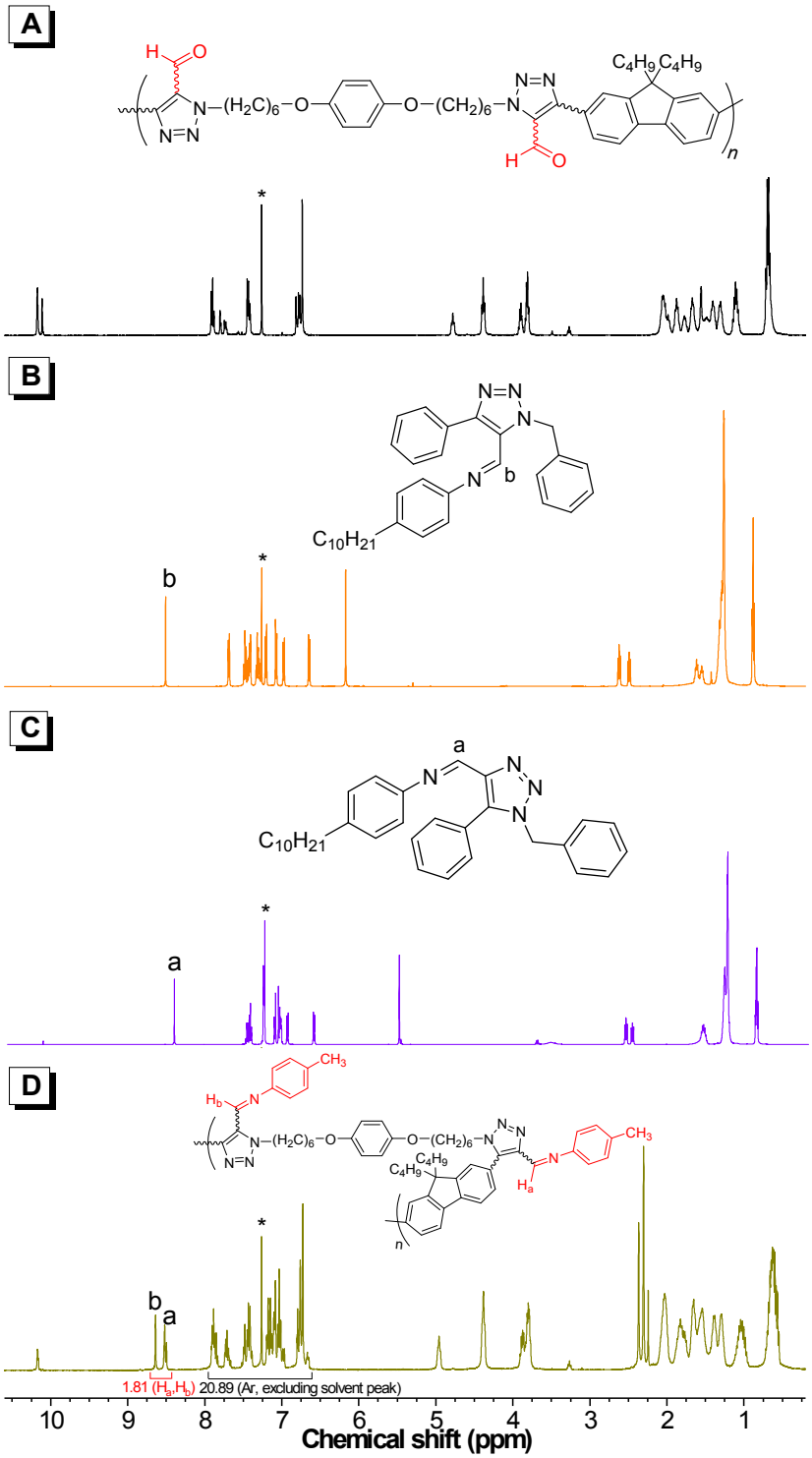

Fig. S18 ^{1}H NMR spectra of P**1a2a** (A), **6**-B (B), **6**-A (C) and **PPM1** (D) in $CDCl_3$. The solvent peaks are marked with asterisks.

The grafting degree of **PPM1** is arranged as x, then un-reacted part accounts for (1-x),

$$\frac{2x}{18x + 10(1-x)} = \frac{1.81}{20.89}$$

$$x = 0.657$$

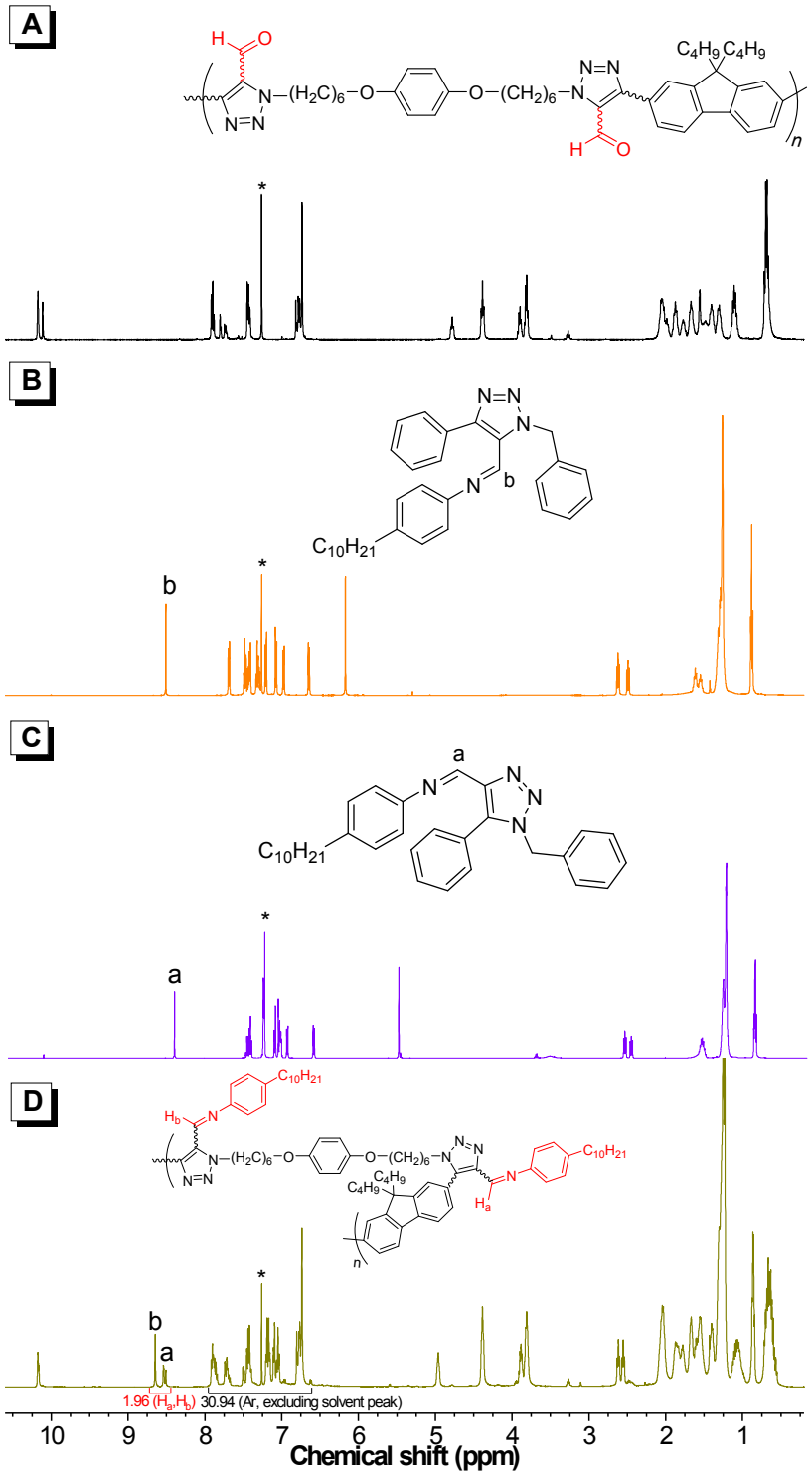

Fig. S19 ^{1}H NMR spectra of P**1a2a** (A), **6**-B (B), **6**-A (C) and **PPM2** (D) in $CDCl_3$. The solvent peaks are marked with asterisks.

The grafting degree of **PPM2** is arranged as x, then un-reacted part accounts for (1-x),

$$\frac{2x}{18x + 10(1-x)} = \frac{1.96}{30.94}$$

$$x = 0.424$$

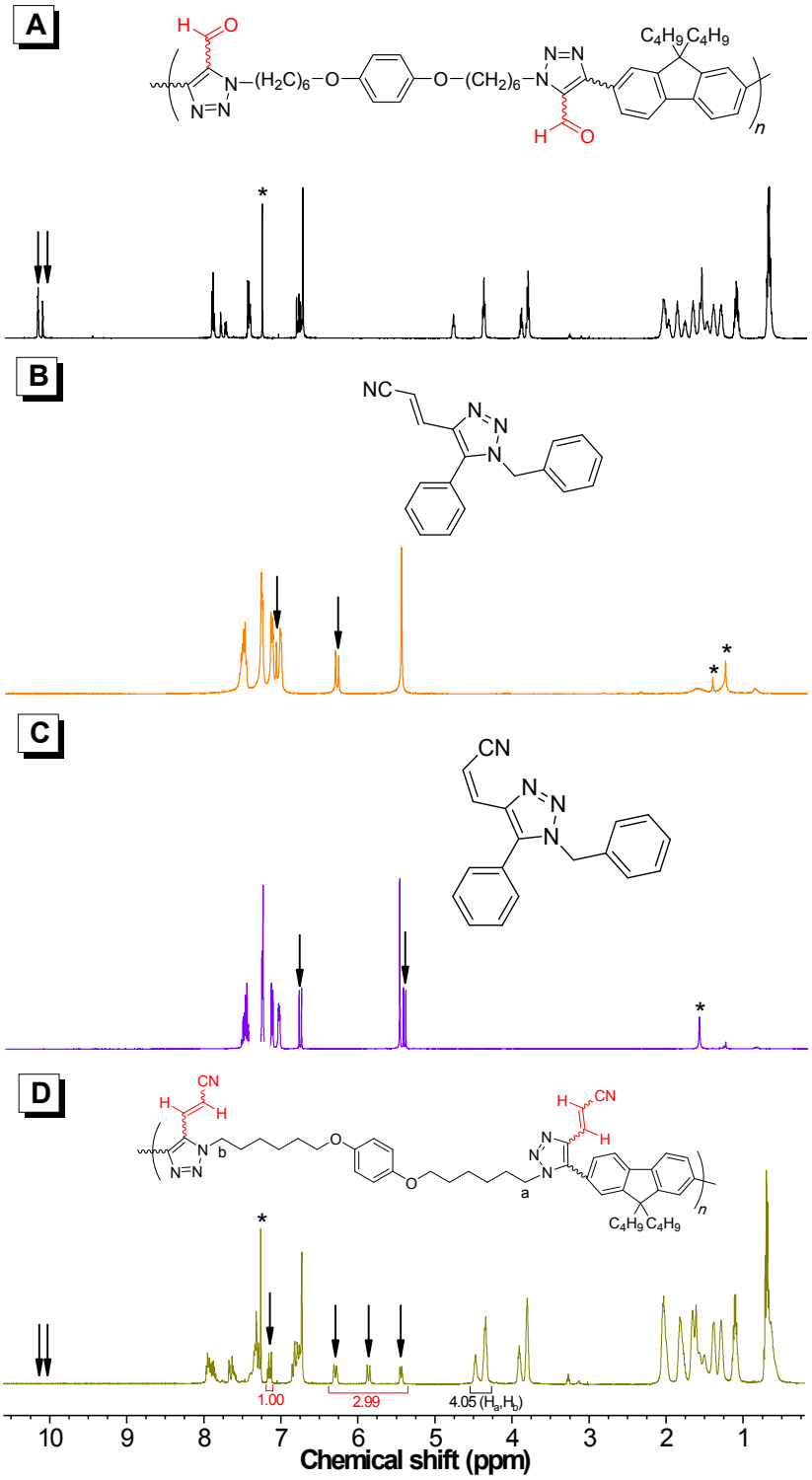

Fig. S20 ^{1}H NMR spectra of P**1a2a** (A), *trans*-**7** (B), *cis*-**7** (C) and **PPM3** (D) in $CDCl_3$. The solvent peaks are marked with asterisks.

The grafting degree of **PPM3** is arranged as x, then un-reacted part accounts for (1-x),

$$\frac{4x}{4} = \frac{3.99}{4.05}$$

$$x = 0.985$$

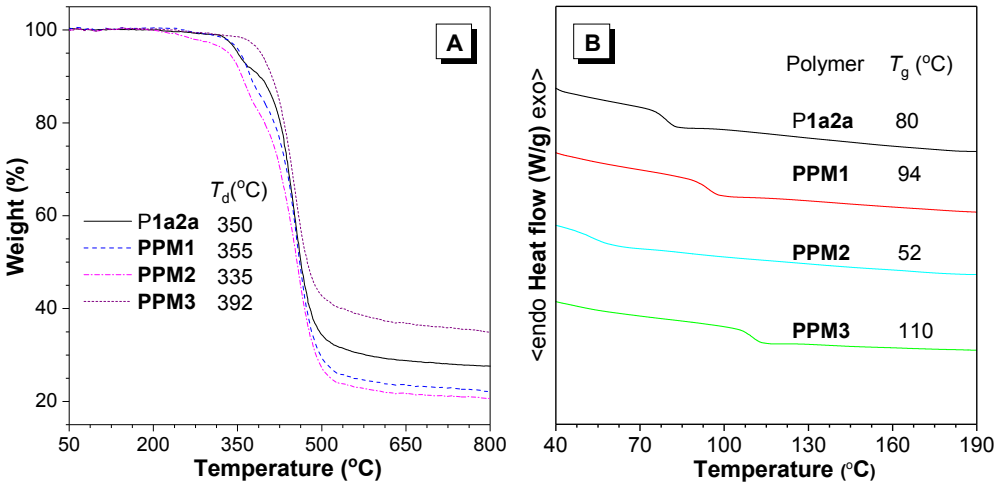

Fig. S21 TGA (A) and DSC (B) curves of P**1a2a** and its derivatives at a heating rate of 20 °C min^{-1} under nitrogen. T_d presents temperature of 5% weight loss.

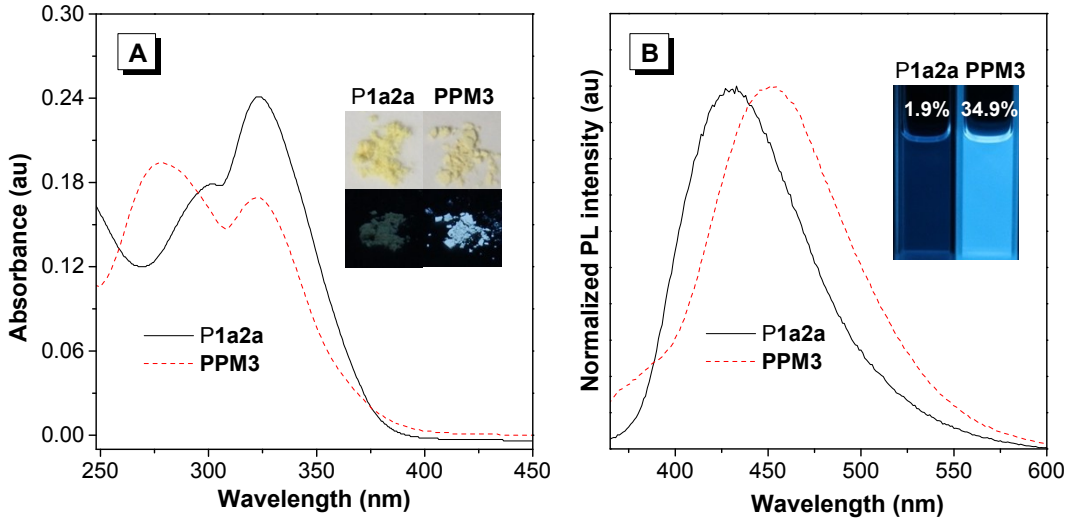

Fig. S22 UV-vis absorption spectra (A) and PL spectra (B) of P**1a2a** and **PPM3** in THF solutions. Concentrations: 10^{-5} M, λ_{ex} = 323 nm. Inset: photographs of P**1a2a** and **PPM3** powders (A) and their THF solutions (B) taken under daylight and UV illumination.

References

(1) X. Lang, F. You, X. He, Y. Yu and L. He, *Green Chem.*, 2019, **21**, 509–514.

(2) J. M. Hoover and S. S. Stahl, *J. Am. Chem. Soc*., 2011, **133**, 16901–16910.

(3) Y. Liu, J. Wang, D. Huang, J. Zhang, S. Guo, R. Hu, Z. Zhao, A. Qin and B. Z. Tang, *Polym. Chem.*, 2015, **6**, 5545–5549.

(4) A. Qin, L. Tang, J. W. Y. Lam, C. K. W. Jim, Y. Yu, H. Zhao, J. Z. Sun and B. Z. Tang, *Adv. Funct. Mater*., 2009, **19**, 1891–1900.

(5) Y. Zhao and T. M. Swager, *Eur. J. Org. Chem*., 2015, **2015**, 4593–4597.

(6) W. Chi, W. Yuan, J. Du, T. Han, H. Li, Y. Li and B. Z. Tang, *Macromol. Rapid Commun.*, 2018, **39**, 1800604.

(7) Y. Wang, W. Wang, X. Wang, X. Cheng, A. Qin, J. Z. Sun and B. Z. Tang, *Polym. Chem.*, 2017, **8**, 5546–5553.

(8) Y. Hu, J. Zhu, K. H. Chan and Y. H. Wong, *Bioorg. Med. Chem*., 2013, **21**, 547–552.